A multi-siderophile element connection between volcanic hotspots and Earth's core

Bradley J. Peters[1]*, Andrea Mundl-Petermeier[2], Valerie A. Finlayson[3]

[1]Institute for Geochemistry and Petrology, ETH Zürich, CH-8092 Zürich, Switzerland
bradley.peters@erdw.ethz.ch

[2]Department of Lithospheric Research, University of Vienna, 1090 Vienna, Austria
andrea.mundl@univie.ac.at

[3]Department of Geology, University of Maryland, College Park, MD 20742, United States
vfinlays@umd.edu

*Corresponding author

Submitted to *Earth and Planetary Science Letters*

Abstract word count: 325

Main text word count: 5893

Tables: 1

Figures: 8

Supplementary figures and tables accompany this article.

Abstract

The existence of resolvable $^{182}W/^{184}W$ deficits in modern ocean island basalts (OIB) relative to the bulk silicate Earth has raised questions about the relationship of these rocks to Earth's core. However, because the core is expected to host high abundances of highly siderophile elements (HSE), it would be expected that such heterogeneity is accompanied by correlating variability in HSE abundances among OIB, but this has not been observed. We report instead a relationship between the W isotopic compositions of Hawai‘i and Iceland OIB, representing two of Earth's primary mantle plumes, and their Ru/Ir ratios. Previous studies have highlighted the unique behavior of Ru relative to Os and Ir during metal-silicate fractionation, particularly when sulfide is segregated with metal. Using the information from these studies, we construct models predicting the consequences for HSE fractionation of various scenarios in which $^{182}W/^{184}W$ deficits can be created. It is shown that the observed trends are likely inconsistent with modern, active core-mantle interaction at the CMB in OIB sources, and instead the observed low-Ru/Ir, low-$^{182}W/^{184}W$ OIB are best explained by metal-silicate interaction that happened at significantly lower pressures. Such conditions reflect what is expected for metal-silicate equilibration during core formation itself, meaning that the deep mantle sources of OIB, such as ultra-low velocity zones, may instead reflect preserved relics of core formation. An ancient origin for core-mantle boundary domains is consistent with geophysical and petrological observations, for example that the Mg/Fe ratio of ferropericlase in the D″ layer is in significant disequilibrium with the modern core. Additional work is required to constrain the behavior of HSE during silicate differentiation processes that may also generate low $^{182}W/^{184}W$ ratios. However, if modern OIB represent a direct link to the ancient processes of core formation, future geochemical studies may be able to unlock new information

about the formation and evolution of the core, as well as the identity and nature of the cosmic building blocks that delivered HSE to Earth during its accretion.

Keywords: mantle plume, core-mantle interaction, metal-silicate equilibration, siderophile elements, tungsten isotopes, early Earth processes

1. Introduction

The largely negative $\mu^{182}W$ ($^{182}W/^{184}W$ normalized to the terrestrial standard, in parts per million) compositions of modern ocean island basalts (OIB; e.g., Rizo et al., 2019; Mundl-Petermeier et al., 2020) stand in stark contrast to the almost exclusively positive $\mu^{182}W$ record of Archean tonalite-trondjemite-granodiorite (TTG) assemblages (e.g., Tusch et al., 2019; Reimink et al., 2020). This apparent discrepancy raises crucial questions about the identity and accessibility of terrestrial mantle domains that host heterogeneous W isotopic signatures at different times in Earth's history. In particular, it has been proposed that OIB mantle sources are distinct from the mantle sources of Archean felsic and mafic rocks. Some OIB sources are thought to contain geochemically detectible proportions of core-equilibrated material (Rizo et al., 2019; Mundl-Petermeier et al., 2020) because the siderophile nature of W means that the core should possess a strongly negative $\mu^{182}W$ if it was formed during the lifetime of the ^{182}Hf-^{182}W system (i.e., prior to ca. 4.5 Ga). In contrast, the common explanation for the positive $\mu^{182}W$ signature of TTG is that it reflects a signature residual to core formation that remained undiluted by W from late accretion at least until TTG precursors were extracted from the mantle (e.g., Mei et al., 2020).

On the other hand, the dominantly positive $\mu^{182}W$ record from the Archean is not universal. Felsic and mafic-ultramafic rocks from southern Africa possess negative $\mu^{182}W$ signatures (Puchtel et al., 2016a; Tusch et al., 2022), consistent with a prior survey of glacial diamictites in the same region (Mundl et al., 2018). Additionally, some Archean-aged komatiites also possess negative $\mu^{182}W$ signatures (Touboul et al., 2012; Puchtel et al., 2016b, 2020). Thus, one alternative explanation for the negative $\mu^{182}W$ of modern OIB is that they have mantle sources with histories like those of some Archean rocks, and that these sources have survived for >2.5 Ga. In the case of komatiites, these signatures are often proposed to derive from core-mantle interaction or heterogeneous preservation of late-accreted components (e.g., Puchtel et al., 2020). For some mafic and felsic rocks, it was alternatively proposed that >4.5 Ga restites to TTG formation represent a domain with negative $\mu^{182}W$ signatures that could be recycled into the mantle source of Archean lavas (Tusch et al., 2022). Given that W is only moderately siderophile, it is also possible that differences in $\mu^{182}W$ compositions arise as a result of other Hadean-aged mantle differentiation events, including magma ocean crystallization (e.g., Brown et al., 2014; cf., Puchtel et al., 2016b).

One geochemical factor capable of distinguishing these hypotheses is the behavior of highly siderophile elements (HSE: Os, Ir, Ru, Pt, Pd, Re). The properties of these elements means that they are strongly enriched in metal-rich domains, such as planetary cores, and correspondingly depleted in silicate domains. This poses some challenges for hypotheses that invoke core-mantle interaction in OIB sources because there is no observed link between HSE abundances and W isotopic compositions in these rocks. The discovery of such a link may be made analytically difficult by lower-than-expected HSE abundances in mantle domains that have equilibrated with the core (Mundl-Petermeier et al., 2020), however relatively low mantle HSE abundances compared to the core may counteract this effect. Additionally, low-degree mantle melts like OIB are susceptible to changes in their HSE abundances during magma differentiation, both due to fractional crystallization (FC) and sulfur saturation (e.g., Keays & Lightfoot, 2007), and this obscures the HSE composition of OIB sources. On the other hand, if the existence of a dynamic link between Earth's mantle and core could be proven, this would strongly influence global models of processes such as late accretion (Peters et al., 2021), the thermal evolution and secular convection of Earth's mantle, and extant understanding of intra-core dynamics (e.g., Brandon &

Walker, 2005). More detailed understanding of any potential links between W, HSE, and Earth's core is, therefore, critical to interrogating this hypothesis for the generation of negative $\mu^{182}W$ signatures in modern OIB.

An important observation that has arisen from experimental and observational studies is that it is unlikely HSE are equally siderophile during metal-silicate equilibration. Mann et al. (2012) reported that Ir is more strongly siderophile than Ru and Pt more strongly siderophile than Pd over a range of pressures and temperatures that are expected during core formation. Laurenz et al. (2016) extended this experimental observation to show that the presence of sulfur acts to make HSE less siderophile and increases the tendency for the silicate residue to preferentially retain Ru and Pd relative to Ir. Terrestrial core formation therefore likely led to elevated Ru/Ir and Pd/Ir ratios in Earth's mantle relative to chondrites, and relative to the core itself. Late accretion of material with chondritic HSE abundances would have diluted these relative enrichments. However, at predicted mass fractions of late accreted material (e.g., Walker, 2009), they would likely not disappear entirely. This may be one reason why relative HSE abundances in Earth's upper mantle are at least partially non-chondritic (Becker et al., 2006; Paquet et al., 2022; cf., Laurenz et al., 2016) and why some OIB show analogous, but even more extreme relative excesses of Ru and Pd (e.g., Peters et al., 2016). Consequently, the relative abundances of HSE may play an equally, if not more important role than absolute HSE abundances in evaluating the veracity of core-mantle interaction in OIB sources.

2. A tungsten-highly siderophile element link

Consistent with this notion, there are positive relationships between $\mu^{182}W$ and Ru/Ir ratios among Hawai'i and Iceland OIB (**Figure 1**) and an analogous, but more poorly defined relationship between $\mu^{182}W$ and Pd/Pt ratios among Hawai'i OIB (**Figure S1**). The slopes of these relationships are distinct for each island, a trait reminiscent of their distinct $^{3}He/^{4}He$-$\mu^{182}W$ trends (Mundl-Petermeier et al., 2020) and the general isotopic systematics of many multi-island hotspot chains (e.g., Weis et al., 2020). The existence of such relationships is *a priori* evidence against a strong effect of mantle melting and magma differentiation on HSE abundance ratios because melting and differentiation have no known effect on W isotopic ratios. This means that significant alteration of HSE abundance ratios by these processes would act to mitigate and eventually erase the observed relationships. However, melting and differentiation processes should still be carefully considered in order to determine whether the observed relationships reflect their respective mantle sources.

The most common mineral phases affecting HSE abundances during melting and magma differentiation are sulfides. Major changes in HSE abundances and intra-HSE ratios arises during sulfur saturation in magmas, which can occur as FC and assimilation of felsic country rocks drive magmatic MgO to lower levels (typically $\leq$ 6 wt.%; e.g., Keays & Lightfoot, 2007; Jamais et al., 2008). All samples for which HSE and W isotopic data are available have MgO > 6 wt.% and do not reflect the very high Ru/Ir ratios (> 5) associated with some OIB containing low MgO (e.g., **Figure 2**). However, relationships between Ru/Ir ratios and indices of FC, such as Ni and MgO are clearly visible among Hawai'i OIB across all MgO contents (**Figure 2a-b**). A correction for FC is therefore applied to all HSE data. In order to accomplish this, representative liquid lines of descent (LLD) for each hotspot are constructed with Petrolog (Danyushevsky & Plechov, 2001) using liquid compositions calculated with PRIMELT3 (Herzberg & Asimow, 2015) from selected primitive samples. The LLD were then post-processed using a variety of available HSE partition coefficients (e.g., Chazey & Neal, 2005; Puchtel & Humayun, 2001; **Figure 2a**) to calculate the evolution of Ru/Ir ratios during FC. Based on the fit to the observed correlations, the partition coefficients of Puchtel & Humayun (2001) were selected to perform the correction. Liquid compositions for each sample were then calculated by olivine addition or subtraction using PRIMELT3 and the results were post-processed to calculate analogous changes in Ru and Ir abundances during FC. Although PRIMELT3 is not capable of reconstructing FC involving phases other than olivine, changes in HSE abundances during FC are primarily controlled by precipitation of trace sulfide phases, which are almost exclusively hosted by olivine phenocrysts. Thus, additional precipitation of clinopyroxene, as sometimes detected by PRIMELT3, will not affect the FC correction. Samples that do not return solutions in PRIMELT3 were filtered out of the dataset.

This correction essentially eliminates the dependence of Ru/Ir ratios on MgO and Ni in the case of Hawai‘i and Iceland OIB (**Figure 2c-d**); the corrected Ru/Ir ratios for both hotspots are displayed in **Figure 1c-d**. For Hawai‘i OIB, a possible residual trend between MgO and Ru/Ir ratios is still evident for MgO abundances less than ca. 12 wt.%, although it is less pronounced than before the correction is applied. However, all Hawai‘i OIB with HSE and W isotopic data have MgO contents > 14 wt.%, meaning that such a trend, if it exists, will not affect the relationships observed in **Figure 1**. In addition, in-situ studies of HSE abundances among silicate, oxide, and sulfide phases have revealed no significant potential for the crystallization of these phases to change magmatic Ru/Ir ratios during magma differentiation (e.g., Gannoun et al., 2016, and references therein). Thus, it is considered unlikely that there are significant FC effects not captured by the correction.

Further, the relationships shown in **Figure 1** overlap with Réunion OIB compositions, which generally have high MgO abundances and whose Ru/Ir ratios were inferred to be unaffected by FC on the basis of *in situ* HSE abundance measurements (Peters et al., 2016).

In Earth's mantle, HSE compositions can be changed dramatically through partial melting, usually though incomplete exhaustion of base metal sulfides (BMS) and metal alloys. In general, research studying the effect of these phases on HSE abundances during mantle melting focuses on fractionation between iridium-group platinum group elements (IPGE: Os, Ir, Ru) and palladium-group platinum group elements (PPGE: Pt, Pd) and have not reveled compelling evidence for strong intra-IPGE fractionation during melting of degrees typical for OIB (< 20%) (e.g., Mungall & Brenan, 2014; Lorand et al., 2010; Luguet et al., 2007). Similarly, the *in situ* data of Alard et al. (2000) for peridotites display no systematic bias of either silicate-hosted BMS or interstitial sulfides to Ru/Ir ratios that are distinct from primitive mantle estimates. On the other hand, some studies (Luguet et al., 2007; Lorand et al., 2010) have reported that some BMS may have a slight preference for Ru relative to Ir. This raises the possibility that heterogeneous Ru/Ir ratios may arise in OIB parental magmas that derive from variable degrees of partial melting. The integrated effect of this preference, if it systematically exists, could produce measurable differences in the Ru/Ir ratios of mantle domains with distinct melt extraction histories. However, Paquet et al. (2022) demonstrated that there is no relationship between bulk-rock Al_2O_3 abundances, a sensitive tracer of time-integrated mantle melting, and Ru/Ir ratios among global abyssal peridotites. A study observing the effect of mantle melting on HSE in arc environments (Dale et al., 2012) similarly found no compelling evidence for Ru-Ir fractionation by mantle melting. Among global OIB, there is no apparent relationship between Ru/Ir ratios and typical indicators for the degree of mantle source melting (e.g., La/Yb, TiO_2, total alkali; **Figure 3**). In contrast, many studies have found strong evidence for fractionation of Pd/Ir and Pd/Pt ratios during mantle melting due to the distinct behavior of these elements in BMS and alloys (e.g., Mungall & Brenan, 2014; Luguet et al., 2007). Consequently, the relationship between W isotopic compositions and Pd/Pt ratios (**Figure S1**) is not discussed further. On the other hand, the observed relationship between $\mu^{182}W$ and Ru/Ir ratios is interpreted to not have changed substantially due to OIB source melting or magma differentiation and instead is interpreted to represent an OIB source feature.

3. A model for the origin of negative-μ^{182}W, low-Ru/Ir OIB magmas

The observed relationship between W isotopic compositions and Ru/Ir ratios can be described as representing a mixing relationship between two mantle domains: one with negative $\mu^{182}W$ and subchondritic (<1.5) Ru/Ir and a second with $\mu^{182}W$ near zero and suprachondritic Ru/Ir (≥ ca. 3.8). It is hypothesized that variable Ru/Ir ratios in OIB sources may reflect the variably siderophile and chalcophile behavior of Ru and Ir during early metal-silicate equilibration (Mann et al., 2012; Laurenz et al., 2016), such that certain ancient and modern mantle domains that have experienced metal-silicate equilibration may retain elevated Ru/Ir ratios. By mass balance, the core must possess a chondritic to slightly subchondritic Ru/Ir ratio. Due to the lithophile nature of Hf and the contrasting moderately siderophile behavior of W, the core is thought to have a modern $\mu^{182}W$ of approximately -220 (e.g., Kleine & Walker, 2017) whereas the silicate Earth and modern depleted mantle must have a $^{182}W/^{184}W$ close to the terrestrial standard (i.e., $\mu^{182}W \approx 0$; Mundl et al., 2017; Budde et al., 2022). Thus, suprachondritic Ru/Ir ratios are likely associated with $\mu^{182}W$ compositions of approximately 0 in the bulk mantle, and chondritic to subchondritic Ru/Ir ratios may be associated with negative $\mu^{182}W$ in Earth's core and silicate domains that have equilibrated with it.

The exact mechanism of core-mantle exchange that would produce these core-equilibrated silicate domains is under debate (see Hernlund & McNamara, 2015, for a review). Many volcanic hotspots have been identified to overlie seismically anomalous regions of the mantle known as large low shear velocity provinces (LLSVP) or ultra-low velocity zones (ULVZ) that are commonly interpreted to have compositions distinct from the surrounding deep mantle. For example, the internal seismic properties of the Hawaiian ULVZ have been recently suggested to reflect core exsolution that generates progressively more Fe-rich silicate material towards the core-mantle boundary (CMB; Li et al., 2022). This Fe-rich material may also carry siderophile trace elements with distinct HSE compositions. Similarly, exsolution of Si-Fe-Mg oxides from metal (e.g., Humayun, 2011) has been shown in laboratory experiments to preferentially bring W into the oxides while other HSE remain in the metal (Yoshino et al., 2020; Rizo et al., 2019; Shofner et al., 2016; Chabot et al., 2015). These processes may therefore promote the transfer of core-derived W into the mantle without significantly enriching it in HSE and may additionally generate intra-HSE fractionation of variable degrees (cf., Chabot et al., 2015; Mann et al., 2012).

A model considering the potential chemical characteristics of such a core-mantle equilibrated domain (CMED) was constructed using the partition coefficients of Mann et al. (2012) and Schofner et al. (2014) following the framework of Mundl-Petermeier et al. (2020). Mann et al. (2012) is selected primarily because it considers partitioning over a variety of pressures relevant to core formation (cf., Rubie et al., 2011) and because its experimental setup most closely reflects recent seismological observations of CMB activity (Li et al., 2022). Tabulated inputs and results are available in **Table 1**. For input pressures between 10 and 135 GPa (i.e., modern CMB pressure) and temperatures fixed to 100 K above the mantle solidus (using the chondritic mantle equation of Simon & Glatzel, 1929), calculated Ru/Ir in the CMED varies from 6.7 to 14 and calculated W abundance varies from 5.0 to 310 ppb (**Figure 4a**). Similarly, for pressures fixed to 50 (representing an average pressure of metal-silicate equilibration during core formation; cf., Fischer et al., 2015) or 135 GPa and temperatures varied from 200 K below to 2000 K above the mantle solidus, calculated Ru/Ir decreases from 21 to 2.2 (50 GPa) or from 16 to 1.0 (135 GPa; **Figure 4b-c**). In the same scenario, W abundances in the CMED decrease from 660 to 34 ppb or 66 to 4.5 ppb as the temperature is increased at constant pressure. Calculated W abundances are also highly sensitive to input oxidation state, with more reduced conditions leading to lower W abundances in the CMED. For example, for pressures of 50 or 135 GPa and temperatures fixed 100 K above the mantle solidus, W abundances vary from <0.1 to 2500 ppb or from <0.1 to 25000 ppb as CMED ΔIW is varied from -5 to -1 (**Figure 5**). More oxidized conditions also increase the abundances of HSE in the CMED, but they do not strongly change calculated Ru/Ir or other intra-HSE ratios.

The selection of model input thus has a strong impact on the resulting endmember compositions; in particular, there are only some conditions that lead to Ru/Ir ratios as low as what is observed for Hawai‘i or Iceland OIB. For example, a CMED that equilibrated under modern CMB conditions (P = 135.8 GPa, T = 4250K, ΔIW = -2.3) produces very high Ru/Ir (up to >13) compared to OIB (ca. 0.8-3.4), and so mixing between this CMED and an observational OIB endmember (W = 13 ppb, the BSE abundance of Arevalo & McDonough, 2008) produces a mixing curve that trends away from the compiled OIB data (**Figure 6a**). A mixing model between the OIB endmember and a chondritic endmember, which simulates the incorporation of unmixed late accretion components instead of core-equilibrated material (cf., Puchtel et al., 2022, for komatiites) produces a curve that passes through the Hawai‘i OIB data (**Figure 6b)**. Secondary mixing with a DMM-like component (W = 3 ppb; Arevalo & McDonough, 2008; Ru/Ir = 2.2 ±1.2, 1σ; e.g. Paquet et al., 2022) can produce mixing arrays that overlap some of the OIB data (e.g., **Figure 6b**), especially considering the potential heterogeneity of the DMM endmember. However, many Hawai‘i OIB with relatively low $\mu^{182}W$ for a given Ru/Ir ratio, along with some OIB samples possessing very low Ru/Ir, cannot be explained within a three-component mixing system containing variably mixed chondrite. Similarly, while the secondary mixing arrays for modern core-mantle interaction (**Figure 6**) overlap much of the OIB data, they fail to reproduce the observed trends and are therefore considered an unlikely outcome.

Lower Ru/Ir ratios for the CMED can be achieved by lowering the input pressure and/or increasing the input temperature. However, the sub-chondritic Ru/Ir ratios that seem to be required by the OIB data cannot be achieved, even at extremely high temperatures, unless the pressure at which the CMED equilibrated is substantially lower than modern CMB pressures (**Figure 4a**). **Figure 7a** instead shows models in which a CMED equilibrated at 5-60 GPa and fixed temperature (T = 4250 K) and oxidation state (ΔIW = -3) are mixed with the observational OIB endmember. Metal-silicate equilibration under lower pressure conditions echoes the conditions expected for core formation in the early Earth (e.g., Rubie et al., 2011). This suggests that the CMED, rather than being a modern, active domain that chemically exchanges with the core, may have instead formed in the Hadean Earth contemporaneously with the metal-silicate equilibration that eventually led to core formation. Significant metal-silicate interaction after initial equilibration has been experimentally shown to be a likely product of short-term (minute-scale) contact at moderate pressures (12.5 GPa; Otsuka & Karato, 2012). Such an outcome may in fact be a more likely than modern core-mantle interaction given that the Mg/Fe ratio of ferropericlase in the modern D″ and E′ layers is in significant disequilibrium with the modern core (Trønnes et al., 2019, after Frost et al., 2010). If the observed μ^{182}W-Ru/Ir trends indeed reflect early core-mantle interaction, this raises the possibility that the Fe-rich materials in ULVZ at the base of mantle plumes are themselves preserved relics of metal-silicate equilibration during core formation, an idea previously proposed by experimental petrologists (cf., Trønnes, 2010).

If metal-silicate equilibration occurred during the lifetime of the ^{182}Hf-^{182}W system, as is expected for core formation, this could also produce variable Hf/W ratios and therefore variable μ^{182}W in the CMED. **Figure 7b** displays models for the endmember scenario in which a higher resultant Hf/W ratio in the CMED promoted more rapid ^{182}W ingrowth such that its modern composition is only slightly lower than the most unradiogenic modern OIB (for which $\mu^{182}W \geq -25$; e.g., Mundl-Petermeier et al., 2020). Such higher Hf/W ratios could be produced by, for example, variable Hf abundances in the deepest mantle following magma ocean differentiation (cf., Brown et al., 2014). Considering the variability of modern DMM with respect to Ru/Ir ratios, these combinations of input parameters best reproduce the observed OIB trends upon secondary mixing with a DMM-like depleted component (**Figure 7d**). It is therefore evaluated that the observed OIB trends are consistent with an OIB source domain possessing negative μ^{182}W and relatively low Ru/Ir ratios that formed in equilibrium with early fractionated metal, possibly contemporaneously with core formation.

There are several drawbacks to the internal construction of this model. First, generation of the low Ru/Ir ratios required by the OIB data primarily relies on very high input temperatures, from 750 K (60 GPa models in **Figure 7a-b**) to 2000 K (5 GPa models in **Figure 7a-b**) in excess of the mantle liquidus (**Table 1**), when input pressure is lowered below that of the modern CMB. Temperatures equal to or even higher than these have been discussed in the context of metal-silicate equilibration during energetic impact events (Labrosse et al., 2007; Jacobsen et al., 2008). High temperatures may also be required to partition He into the core in quantities large enough to produce the observed He-W isotopic correlations (Yuan & Steinle-Neumann, 2021). However, it is generally predicted that sub-liquidus temperatures are required to explain the abundances of moderately siderophile elements in the terrestrial mantle (e.g., Fischer et al., 2015; Wade & Wood, 2005), in part because very high temperatures promote more oxidized conditions that change metal-silicate partitioning behavior for these elements (cf., Rubie et al., 2011). If basal magma oceans where compositionally and thermally stratified (Laneuville et al., 2018), the requirement for lower temperatures may be satisfied in shallower regions of the magma ocean while thermally insulated deeper regions were able to achieve temperatures high enough to produce the observed Ru/Ir ratios. The data of Mann et al. (2012) indicate that Ru/Ir ratios are not strongly affected by changes in oxidation state (although the abundances of all HSE in the CMED increase under increasingly oxidizing conditions), meaning that in this case a higher oxidation state cannot alleviate the high temperature requirements of this model.

Second, the models in **Figure 7** predict very low W abundances in the CMED (1.2 ppb at 60 GPa to 0.1 ppb at 5 GPa) due to the lower input pressures and oxygen fugacity. This result permits mixing lines that roughly parallel the OIB data trends and substantially higher W abundances (e.g., Mundl-Petermeier et al., 2020) would result in poorer model fits. However, low W abundances require that the mixed OIB source has a very high proportion of CMED material; in **Figure 7d**, where three components are considered, Hawai‘i OIB are predicted to contain ca. 40-90% CMED material depending on input conditions. This constraint may be relaxed when considering newer W partitioning data at high pressures and temperatures, which indicate that W may be less siderophile at the conditions examined by this model (e.g., Blanchard et al., 2022), however no empirical formula directly relating pressure and temperature to W partition coefficients was given in this study. Given these results, the participation of a highly trace-element depleted source domain may seem physically unrealistic, but ‘intrinsic’ deep mantle OIB source domains with similarly depleted compositions have also been previously discussed (e.g., Fitton et al., 2003; DeFelice et al., 2019). Because the CMED is similarly predicted to be depleted in Re and IPGE (Mann et al., 2012), even high mixing proportions of this domain would likely have very little effect on observed abundances of these elements or on the $^{187}Os/^{188}Os$ ratios of OIB. The lack of observed correlations between $\mu^{182}W$ compositions, $^{187}Os/^{188}Os$ ratios, and HSE abundances among OIB is consistent with this conclusion. On the other hand, predicted Pt and Pd abundances in the CMED depicted in **Figure 7** are high (cf., Suer et al., 2021). For example, between 5 and 60 GPa calculated Pt abundances in the CMED increase from 31 to 52 ppb. In this case, the PPGE abundances and Pt/Os ratios of OIB sources could be more strongly affected by incorporation of CMED materials. In general, the PPGE abundances of OIB are notably higher than IPGE abundances (e.g., Waters et al., 2020; Paquet et al., 2019; Ireland et al., 2009), although they do not approach these levels. Further, the notable role of sulfide mineralization in the partitioning behavior of Pt (e.g., Alard et al., 2000) means that such effects may be obscured in measured OIB compositions.

4. Discussion

4.1 *Alternative models generating negative $\mu^{182}W$ in Hadean-Archean domains*

Although at present the idea that negative μ^{182}W compositions in modern OIB are generated by core-mantle interaction is generally accepted (Peters et al., 2021; Mundl-Petermeier et al., 2020; Rizo et al., 2019), there are also alternative models that can generate negative μ^{182}W signatures in the early Earth. In the absence of metal, W behaves as an incompatible trace element with partition coefficients in silicate phases that are generally lower than those of Hf. Thus, silicate differentiation will produce domains with distinct Hf/W ratios, with higher ratios being associated with trace element depleted materials (e.g., solids residual to low-degree partial melting) and lower ratios being associated with trace element enriched materials (e.g., low-degree partial melts). These properties have been developed into two primary models explaining the presence of low μ^{182}W signatures in mantle-derived rocks of Archean age.

First, crystallization of early (≤ ca. 60 Ma after solar system formation) magma oceans is predicted to generate dense (high-Fe), trace element enriched reservoirs with negative μ^{182}W (e.g., Brown et al., 2014) that eventually overturn and could potentially be preserved over long terrestrial timescales near the core-mantle boundary (e.g., Ballmer et al., 2017). Magma ocean crystallization over these timescales would also be predicted to affect the short-lived ^{146}Sm-^{142}Nd isotopic system and produce coupled variations in ^{182}W/^{184}W and ^{142}Nd/^{144}Nd ratios (e.g., Brown et al., 2014). Among Archean mantle-derived rocks, coupled depletions in ^{182}W and ^{142}Nd have been observed in Schapenberg komatiites (Puchtel et al., 2016) and coupled enrichments have been observed in some Isua sample suites (Rizo et al., 2016; Willbold et al., 2011; Caro et al., 2006) although none of these sample sets show $^{182}W/^{184}W$-$^{142}Nd/^{144}Nd$ correlations on a per-sample basis. While modern OIB have strongly variable $^{182}W/^{184}W$, their $^{142}Nd/^{144}Nd$ ratios are close to or barely resolvable from terrestrial standards (e.g., Horan et al., 2018; Peters et al., 2018; Jackson & Carlson, 2012). This first-order observation calls into question whether $\mu^{182}W$ variability in OIB could result from silicate differentiation in an early magma ocean. In addition, because Ru is expected to be less siderophile than Ir during metal-silicate equilibration, the silicate magma ocean would be expected to preserve elevated Ru/Ir ratios residual to core formation (e.g., Laurenz et al., 2016). Such signatures would contrast with the lower Ru/Ir ratios observed among Hawai‘i and Iceland OIB. Although there is a paucity of data indicating how Ru and Ir would behave during subsequent basal magma ocean crystallization, an experimental study of Ru and Os has revealed no significant difference in partitioning among deep-mantle phases (Righter et al., 2020). Since IPGE generally behave similarly during mantle melting, this is *a priori* evidence that Ru/Ir ratios would not be strongly altered by this process. In the case of CMED, the metal-silicate equilibration that led to core formation is expected to occur in a completely molten magma ocean, or in a series of magma oceans (e.g., Rubie et al., 2011) that permit the differentiated, denser metal to percolate beneath silicate liquids. In a completely molten magma ocean following an energetic impact, it may be reasonable to expect that Sm/Nd ratios are efficiently homogenized by rapid convection, and thus that the CMED modeled here would preserve small or undetectable $^{142}Nd/^{144}Nd$ variations (though such variations were likely created in subsequent differentiation events) even though $^{182}W/^{184}W$ heterogeneity is independently generated through metal-silicate interaction. Thus, CMED may be expected to host decoupled ^{142}Nd-^{182}W signatures.

A second process by which negative $\mu^{182}W$ compositions could be created by Hadean silicate differentiation is by recycling of mafic restites to generation of felsic crust. Such a process is attractive because it helps explain trends between ^{182}W and long-lived radiogenic lithophile isotope systems among Archean-aged mafic rocks of the Kaapvaal craton (Tusch et al., 2022). An analogous trend may be present between the ^{182}W and ^{143}Nd (but not ^{176}Hf) compositions of Réunion OIB (Peters et al., 2021), although such trends were not reported in this study. However, the behavior of HSE during this multi-stage process are difficult to predict with extant partitioning data. Felsic upper continental crust (UCC) may have highly elevated Ru/Ir (≥ 10, e.g. Peuker-Ehrenbrink & Jahn, 2001; Schmidt et al., 1997). If the pre-late accretion Hadean mantle possessed more mildly elevated Ru/Ir compared to UCC (e.g., ~3-8, depending on the involvement of S; Laurenz et al., 2016) and formation of mafic protocrust had a negligible effect on Ru/Ir ratios, then by mass balance the restite to felsic crustal formation processes would be expected to have both negative $\mu^{182}W$ (Tusch et al., 2022) and low Ru/Ir. Since mantle melting recorded by abyssal peridotites implies that this process does not change the Ru/Ir ratio of the depleted mantle over time (see Section 2; Paquet et al., 2022), this would mean that generation of Ru/Ir ratios <1.5, as required by the OIB data, would require relatively extreme HSE fractionation during restite formation. Thus, significantly more study of HSE partitioning during early magmatic processes is required to refine this model.

4.2 *The observational OIB endmember: another relic of the early Earth?*

In the model simulating core-mantle interaction, the one OIB endmember is treated as an observational component seated at the upper-right end of the array of Hawai‘i OIB. This endmember is estimated to have Ru/Ir of around 4 (**Figure 8**), which is higher than both chondrites (ca. 1.5; e.g., Horan et al., 2003) and the modern primitive upper mantle (ca. 2.0 ±0.24, 2σ; e.g., Becker et al., 2006). Although the relative HSE abundances of the modern mantle are considered to be roughly chondritic, the difference between the Ru/Ir ratio of the primitive upper mantle and chondrites has been investigated as a relic of a residual, elevated mantle Ru/Ir ratio following core formation (e.g., Laurenz et al., 2016). A simple calculation illustrating the subtraction of chondritic late accretion from modern mantle HSE concentrations also shows that the pre-late accretion mantle would have had a Ru/Ir ratio of 2.9-5.5 for 0.5-0.7% total late accretion by mass (**Figure 8**).

It is broadly expected that the diminishment of positive $\mu^{182}W$ compositions and modern HSE abundances were jointly accomplished through gradual mixing of late accreted components in the mantle over ca. 1.5 Gyr. The composition of the observational OIB endmember could therefore be consistent with an intermediate stage of this process, where the initially higher Ru/Ir ratio of the mantle had mostly diminished and its $\mu^{182}W$ composition had similarly returned to a value near zero. The precise location of this endmember could be more closely investigated by HSE abundance analyses in OIB with zero to slightly positive $\mu^{182}W$ compositions. Regardless of the exact Ru/Ir ratio of this endmember, the existence of two mixing components that each have Ru/Ir ratios dissimilar to the modern mantle raises the question of whether OIB may preserve Ru isotopic compositions reflecting Earth's early building blocks (cf., Fischer-Gödde et al., 2020).

4.3 *Implications of core-mantle interaction in OIB sources*

If core-mantle exchange was active on the early Earth, this may have had consequences for the secular chemical evolution of Earth's mantle. Many of Earth's hotspots are believed to be underlain by mantle plumes, some of which may bring material from the deepest parts of the mantle to the upper mantle and surface (e.g., French & Romanowicz, 2015). If the material at the base of these plumes included core material with negative $\mu^{182}W$, then the integrated flux of plumes from the CMB into the upper mantle may have altered the $\mu^{182}W$ composition of the bulk mantle over geological timescales. The total time-integrated amount of plume material in the mantle can be estimated using the plume flux of the Hawai‘i mantle plume (calculated from the cross-sectional area of the plume swell; Davies, 1992) as an example. Assuming that the 80% of the total plume flux is represented by this swell, that Hawai‘i mantle plume represents 22% of the global flux from the CMB to the bulk mantle (the proportion of buoyancy flux for Hawai‘i compared to all global plumes identified by French & Romanowicz, 2015, as “primary,” or having “clearly resolved,” links to the lower mantle; buoyancy fluxes from Courtillot et al., 2003), and that global plume flux is constant through geological time, approximately 6% of the modern mantle mass derives from plume material originating at the CMB. If this plume material possesses an average $\mu^{182}W$ of -10, it would have lowered the bulk mantle $\mu^{182}W$ by 4.5 ppm over 4.3 Ga (input W abundances identical to Peters et al., 2021). This demonstrates that if core-mantle interaction is a process that operated in mantle plume source domains, it must have a calculable and possibly resolvable effect on global siderophile element compositions over geological time. However, this calculation is likely a minimum estimate because it does not consider plumes originating from the CMB that are poorly imaged by seismic tomography and plumes that stagnate before reaching the surface but are nevertheless mixed into the convicting mantle. Additionally, higher Archean mantle potential temperatures (e.g., Herzberg et al., 2010) may have driven higher plume fluxes than what is observed in the modern mantle and enhanced this plume mixing effect.

The veracity of core-mantle interaction has many additional geophysical consequences. For example, the thermal conductivity of the outer core would likely have resulted in net heat production during early metal-silicate interaction at the base of a magma ocean, which may have sustained core convection and the geodynamo prior to inner core crystallization (Trønnes et al., 2019). Core-mantle exchange over a liquid metal boundary may additionally mediate electromagnetic effects and exert control over the velocity of Earth's rotation and therefore over day length (Buffet et al., 2002). Such considerations warrant further development of the type of geochemical signatures expected from core-mantle interaction and investigation into how geochemical and geophysical signatures of this interaction can be used to study the origins and evolution of core material itself.

5. Summary and Conclusions

A trend between the $\mu^{182}W$ compositions and Ru/Ir ratios of Hawai'i and Iceland OIB is reported and evaluated to be a mantle source feature of these ocean islands. The trend is interpreted to result from core-mantle interaction that occurred at pressures lower than the modern CMB, as this would lead to relatively high Ru/Ir ratios that are not observed among OIB. The lower pressure conditions required to reproduce the observed trends are similar to those expected for core formation, meaning that the envisaged core-mantle interaction may have occurred at the same time as the metal-silicate equilibration that originally formed Earth's core. Additionally, the elevated Ru/Ir ratios recorded by OIB with $\mu^{182}W$ near zero may also reflect an ancient reservoir in the OIB mantle sources. Alternatively, the observed trends may have been generated during Hadean crust formation processes, however additional information regarding the partitioning behavior of HSE is required to evaluate these scenarios. The observed trends strengthen current discussion that OIB act as modern links to Earth's core. Additional study of other siderophile elements and their embedded isotope systems in this framework may unlock more information about the formation and evolution of the terrestrial core, as well as about the siderophile building blocks of the Earth.

Acknowledgements

Support for this research was provided by ETH Zürich/Marie Skłodowska-Curie Actions COFUND (18-1 FEL-28 to BP), the Swiss National Science Foundation (PZ00P2_180005 to BJP), the Austrian Science Fund (V659-N29 to AMP), and the United States National Science Foundation (NSF-EAR 2019856 to VAF). These funding sources are gratefully acknowledged.

Table 1. Summary of model inputs and outputs. For all low-$\mu^{182}W$ endmembers with siderophile element abundances calculated according to Mann et al. (2012) and Schofner et al. (2014), input pressure, temperature, and oxidation state are given. For a chondritic low-$\mu^{182}W$ endmember (**Figure 6b**), HSE abundances are from Horan et al. (2003) and W abundance and isotope composition are from Kleine & Walker (2017). The "OIB mantle," endmember represents the observational endmember discussed in the text and has a Ru/Ir fixed based on a regression of the Hawai'i OIB data (**Figure 8**) with an Ir abundance reflecting the primitive upper mantle value of Becker et al. (2006) and a W abundance reflecting the bulk silicate Earth value of Arevalo & McDonough (2008). The mid-Atlantic ridge (MAR) depleted mid-ocean ridge basalt mantle (DMM) endmember represents sample 11R-1/55.46 of Marchesi et al. (2013), a fixed Ir abundance of 1 ppm, and the DMM W abundance of Arevalo & McDonough (2008). The choice of all other input parameters is discussed in the text.

		Low-$\mu^{182}W$ endmember of						Other endmembers	
		Fig. 6a	**Fig. 6b**	**Fig. 7a**		**Fig. 7b**		**OIB mantle**	**MAR DMM**
Inputs	**Pressure (GPa)**	135.8		5	60	5	60		
	Temperature (K)	4250		4250	4250	4250	4250		
	Oxidation state (ΔIW)	-2		-3	-3	-3	-3		
	Ru/Ir		1.5					4	0.76
	Ir, ppm		0.44395					0.0035	0.001
	$\mu^{182}W$	-220	-240	-220	-220	-35	-35	0	0
	W, ppm		0.093					0.013	0.003
Outputs	**Ru/Ir**	13		0.56	2.1	0.56	2.1		
	Ir, ppm	0.00074		0.000061	0.00011	0.000061	0.00011		
	Ru, ppm	0.0094		0.000034	0.00022	0.000034	0.00022		
	Pt, ppm	0.19		0.032	0.053	0.032	0.053		
	Re, ppm	0.00017		0.0000085	0.000018	0.0000085	0.000018		
	W, ppm	0.90		0.00010	0.0012	0.00010	0.0012		

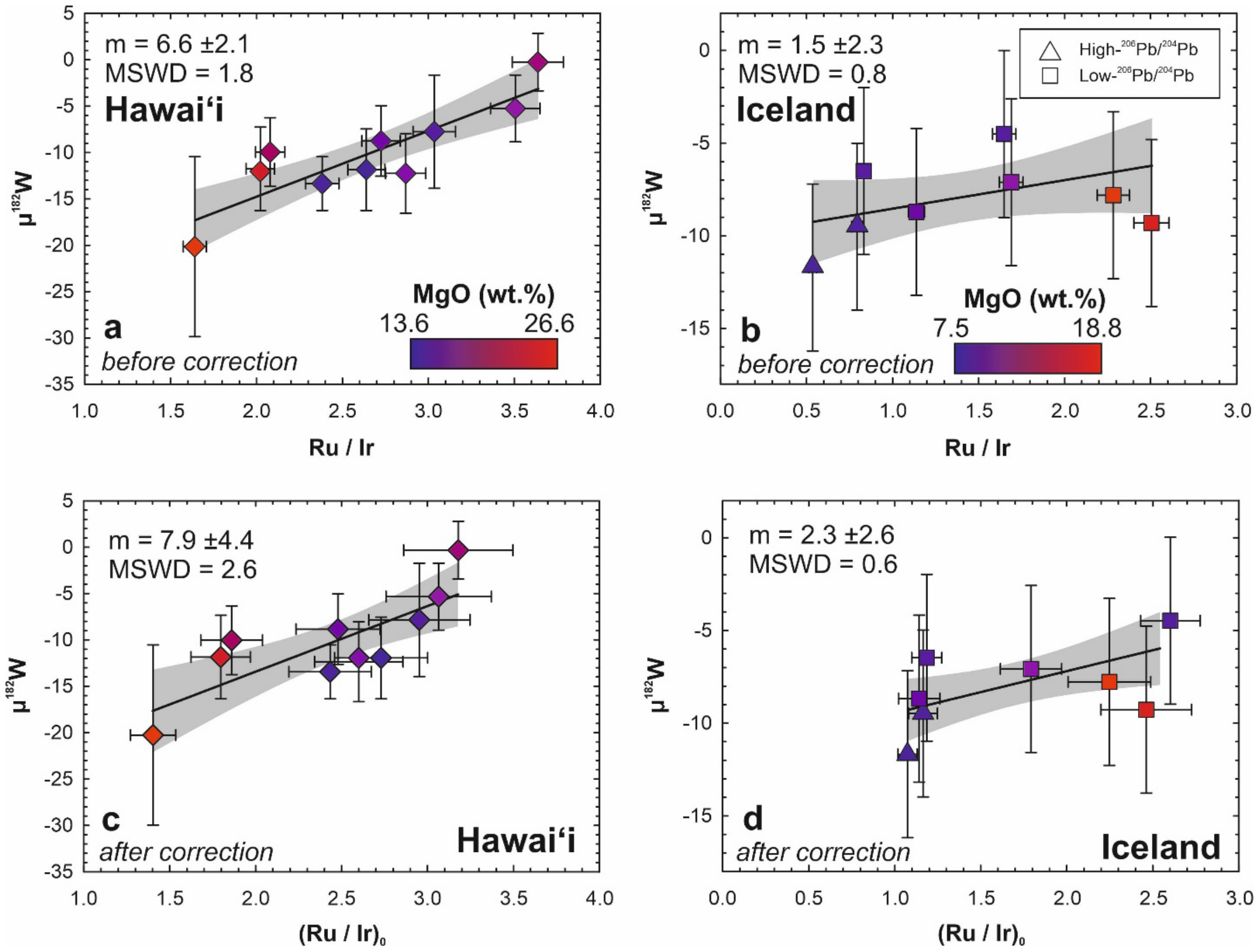

Figure 1. Measured Ru/Ir ratios (panels a-b) and fractional crystallization-corrected Ru/Ir ratios (panels c-d) versus μ^{182}W compositions for Hawai'i and Iceland OIB. Symbols are colored according to the MgO contents of the sample. For Iceland OIB, symbols are differentiated for the 'high-' and 'low-^{206}Pb/^{204}Pb' trends of μ^{182}W vs ^{3}He/^{4}He to illustrate that this difference is not reflected in these trends. In future figures, only square symbols are used for Iceland OIB. Trend statistics are calculated using Isoplot (Ludwig, 2003); uncertainties on slopes represent 95% confidence intervals. Data sources: Mundl-Petermeier et al., 2020, 2019; Mundl et al., 2017; Ireland et al., 2009.

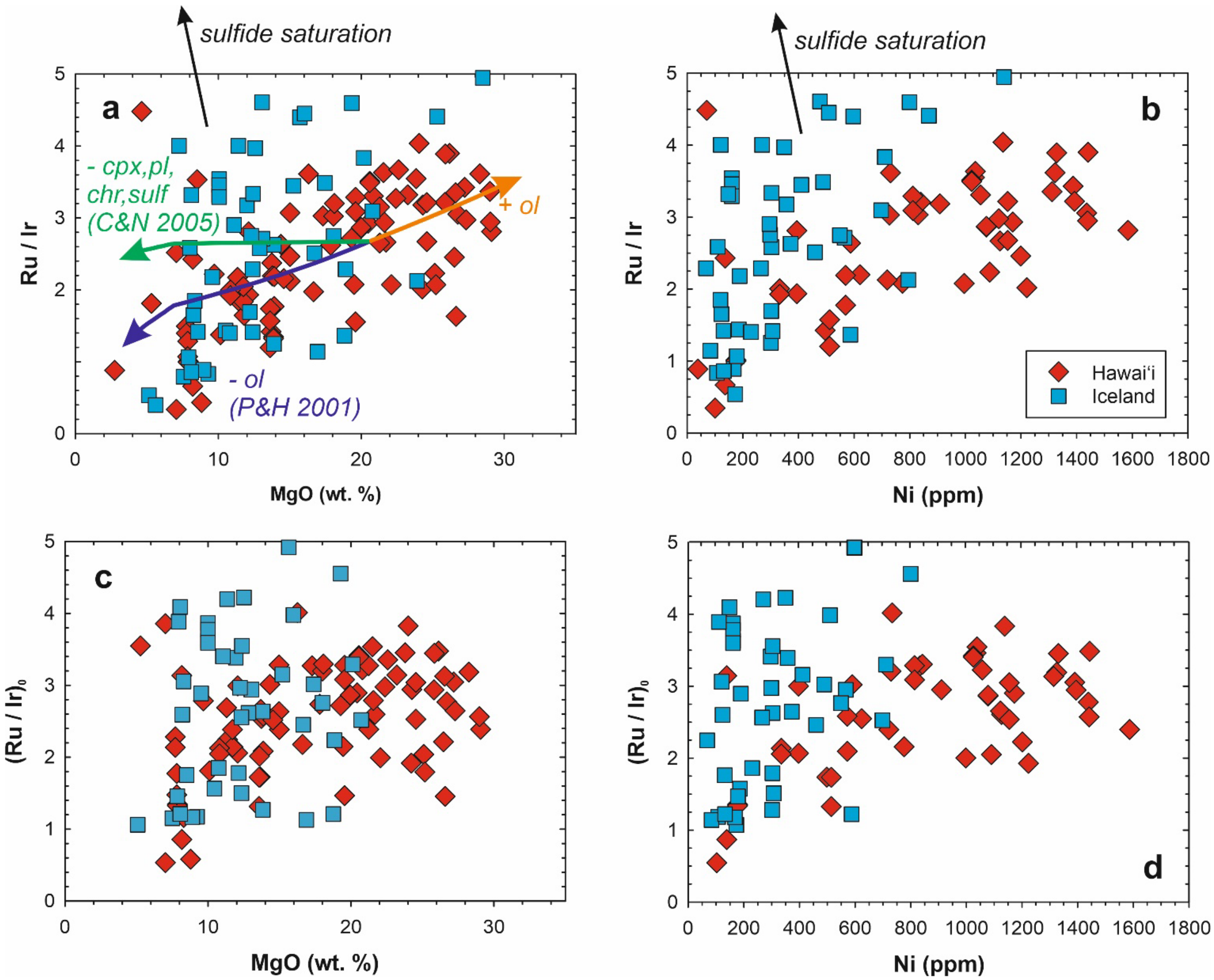

Figure 2. MgO (panels a, c) and Ni (panels b, d) versus measured Ru/Ir ratios (panels a, b) and $(Ru/Ir)_0$ (fractional crystallization-corrected Ru/Ir ratios; panels c, d). Clear relationships between measured Ru/Ir ratios, MgO and Ni are visible in panels a and b. In panel a, these follow the fractional crystallization trends calculated using partition coefficients from Puchtel & Humayun (2001) better than those calculated using partition coefficients from Chazey & Neal (2005). The applied correction for fractional crystallization processes essentially removes visible correlations for Hawai‘i and Iceland OIB. For Hawai‘i OIB, all samples with published HSE and W isotopic data have MgO > 14 wt.%. All available data are included in the figure, regardless of availability of $\mu^{182}W$ compositions for the same sample. For data sources see tables S4 and S5. Data for other hotspots are excluded for clarity.

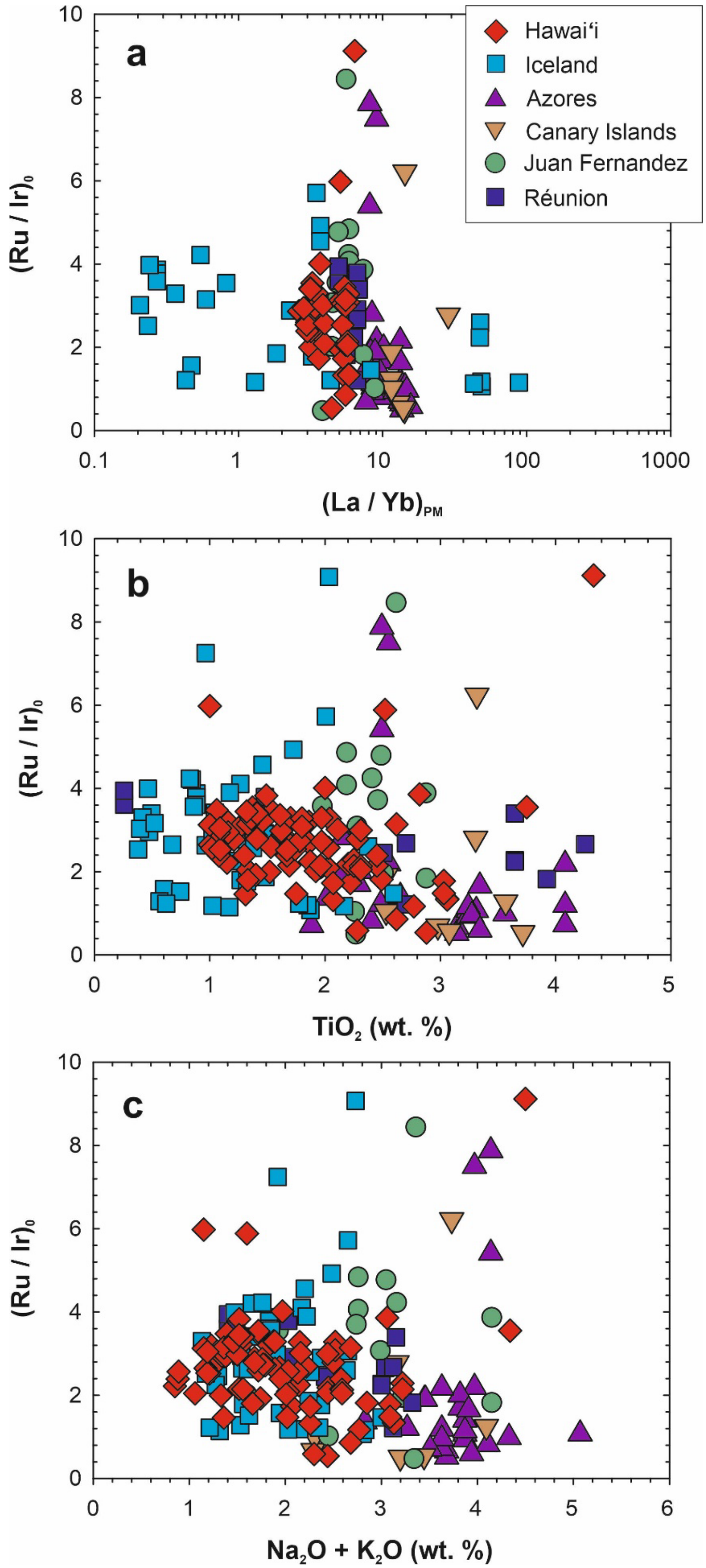

Figure 3. Fractional crystallization-corrected Ru/Ir ratios versus primitive mantle (McDonough & Sun, 1995) normalized La/Yb ratios, TiO_2 compositions, and total alkali contents ($Na_2O + K_2O$), which are common tracers of partial melting degree among intraplate basalts. No global or per-hotspot dependence is observed on a scale that would substantially affect the correlations observed in **Figure 1**. Data sources are listed in the Supplementary Tables.

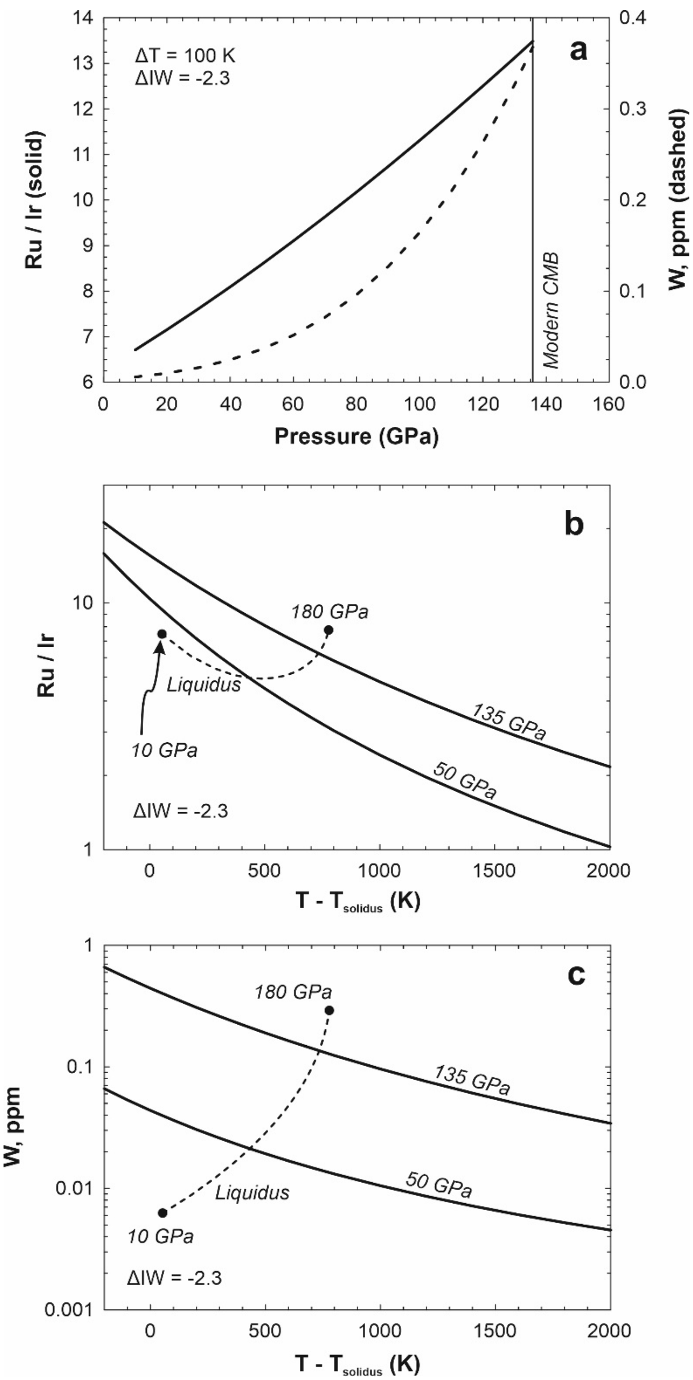

Figure 4. Calculated Ru/Ir ratios and W abundances for variable pressure (panel a) and temperature (panels b, c) inputs. In panel a, the temperature is set to 100K above the solidus temperature for all calculated points. In all panels, the oxidation state is set to IW minus 2.3 log units to simulate conditions intermediate to early (lower oxidation state) and modern (higher oxidation state) core-mantle interaction. In panels b and c, the calculated Ru/Ir ratios for each point along the mantle liquidus are calculated for pressures from 10 to 180 GPa (dashed lines) and intersect the model curves for 50 and 135 GPa at their respective liquidus temperatures. Mantle solidus and liquidus temperatures are calculated from Simon & Glatzel (1929).

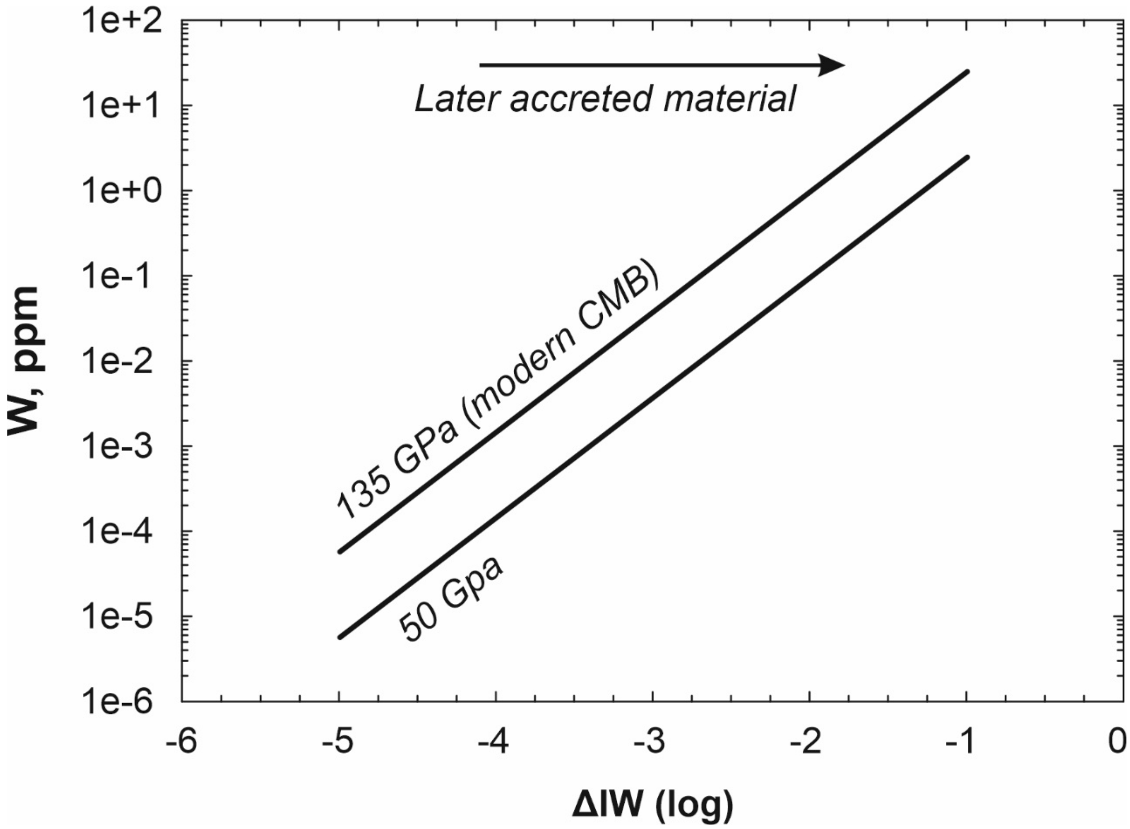

Figure 5. Calculated W abundances in the core-mantle equilibrated domain (CMED) for variable oxidation states at pressures representing the modern core-mantle boundary (CMB) and the average pressure of core formation based on mantle abundances of moderately siderophile elements (ca. 50 GPa; e.g., Fischer et al., 2015). Tungsten is generally more siderophile at lower pressures and under more reducing compositions.

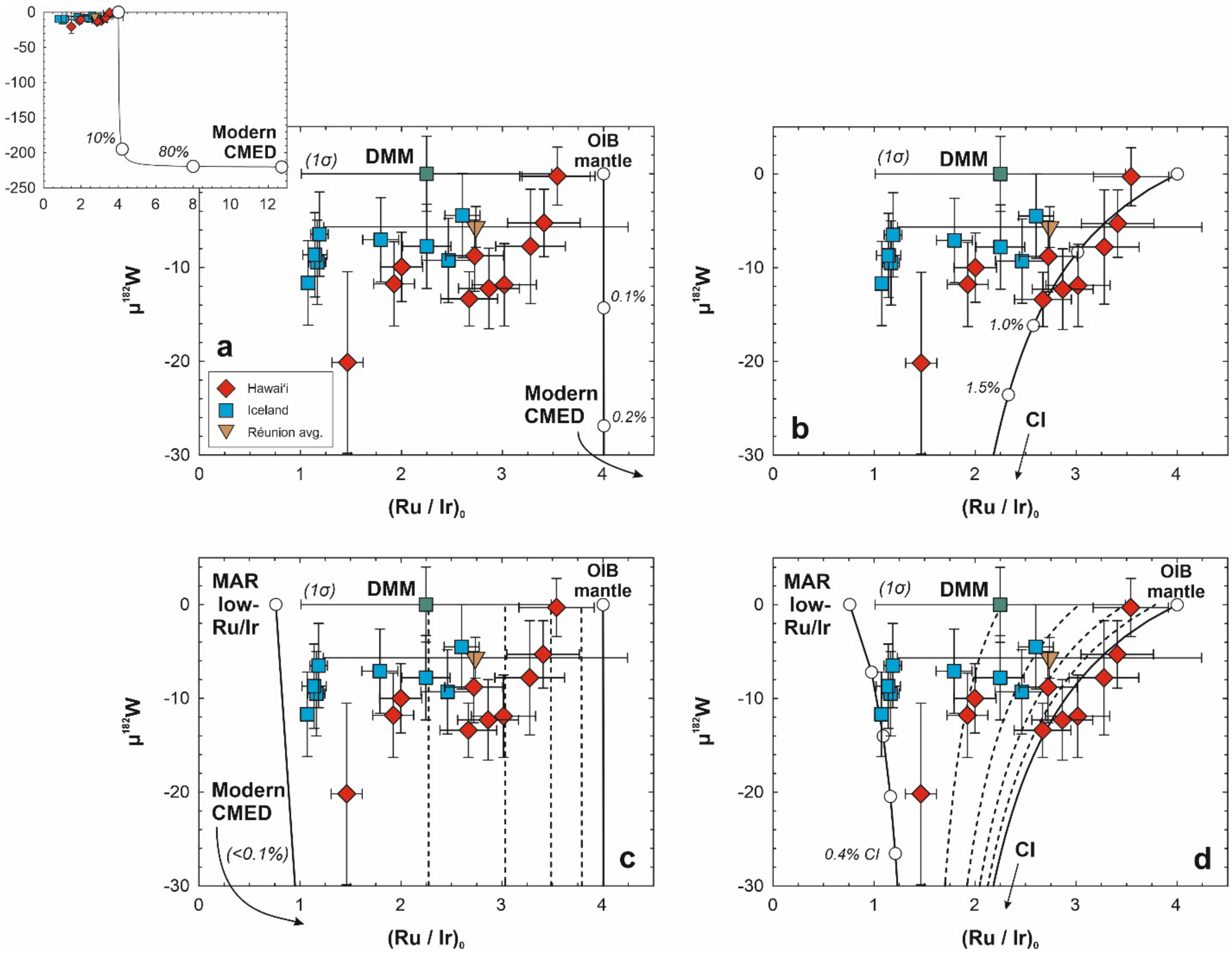

Figure 6. Mixing models between an observational OIB mantle endmember ("OIB mantle") with $\mu^{182}W = 0$ and $Ru/Ir \approx 4$ and calculated low-$\mu^{182}W$ endmembers: a core-mantle equilibrated domain (CMED) formed at the modern core-mantle boundary (CMB; panel a) and unmixed chondritic components left over from late accretion (panel b). The percent proportion of these low-$\mu^{182}W$ reservoirs is given along the bold mixing lines. An inset to panel A shows the position of the modern CMED relative to the data. In panels c and d, these mixing lines are subjected to secondary mixing with a depleted mid-ocean ridge basalt endmember with a low Ru/Ir ratio (after sample 11R-1/22.99 of Marchesi et al., 2013; W = 3 ppb after Arevalo & McDonough, 2008, Ir = 1 ppb). Réunion OIB data are from Peters et al. (2021) and reference DMM composition is an average of fresh abyssal peridotites from Day & Brown (2021). In general, the secondary mixing lines overlap most of the OIB data but fail to reproduce the shapes of the trends. Model inputs and outputs are summarized in **Table 1**. Original data sources for OIB are given in the Supplementary Tables. Reference DMM composition is the average of fresh abyssal peridotites from Day & Brown (2021); all other endmember compositions listed in **Table 1**.

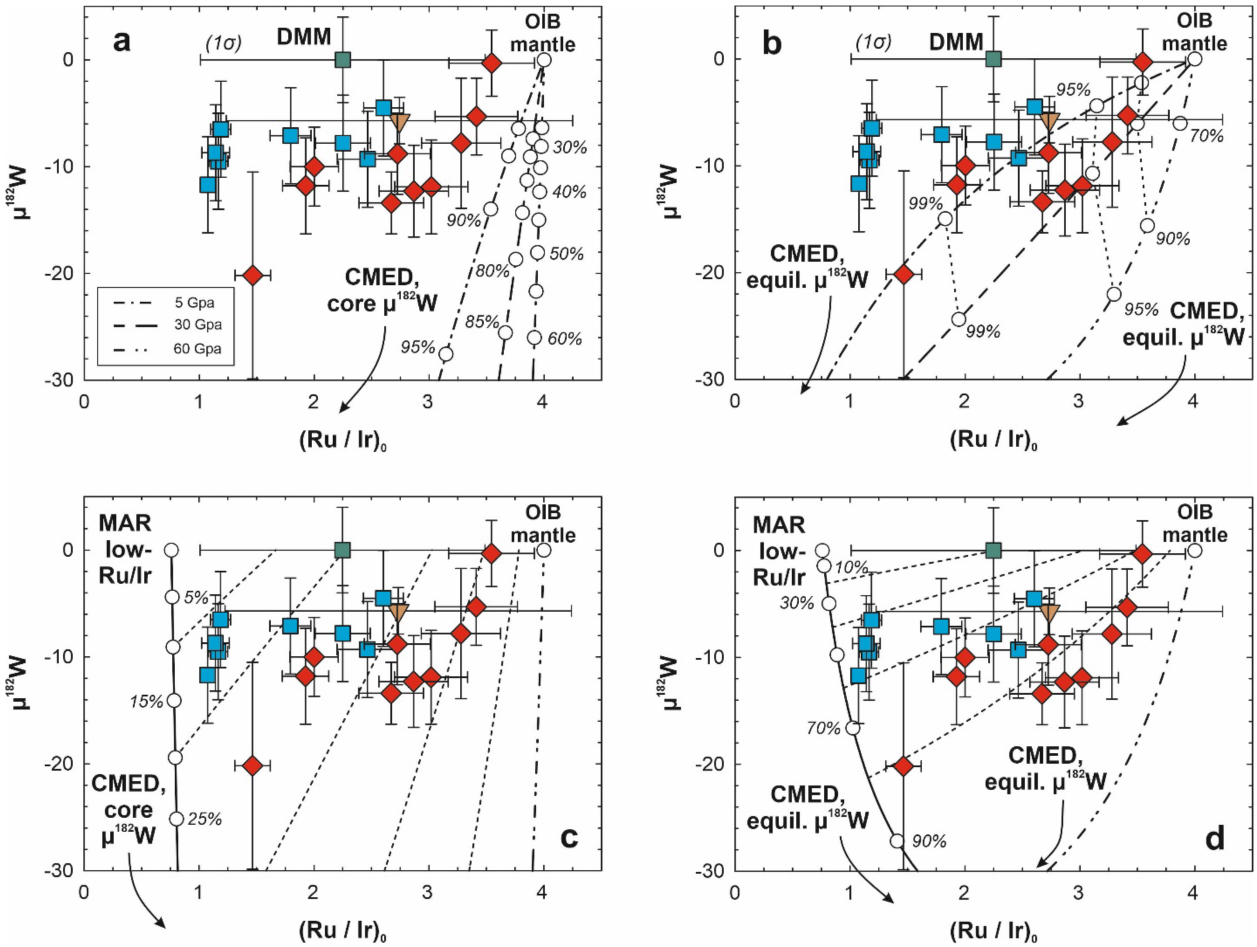

Figure 7. Additional mixing models between an observational OIB mantle endmember ("OIB mantle") with $\mu^{182}W = 0$ and Ru/Ir ≈ 4 and calculated low-$\mu^{182}W$ endmembers: a CMED equilibrated at 5-60 GPa and with either core-like $\mu^{182}W$ (panel a) or equilibrated $\mu^{182}W$ (panel b; see text for details). Secondary mixing lines with depleted mantle materials analogous to those in **Figure 6c-d** are illustrated in panels c and d. It is evaluated that the secondary mixing lines in panel d best reflect the observed data trends. Model inputs and outputs are summarized in **Table 1**. Original data sources for OIB are given in the Supplementary Tables. Reference DMM composition is the average of fresh abyssal peridotites from Day & Brown (2021); all other endmember compositions listed in **Table 1**.

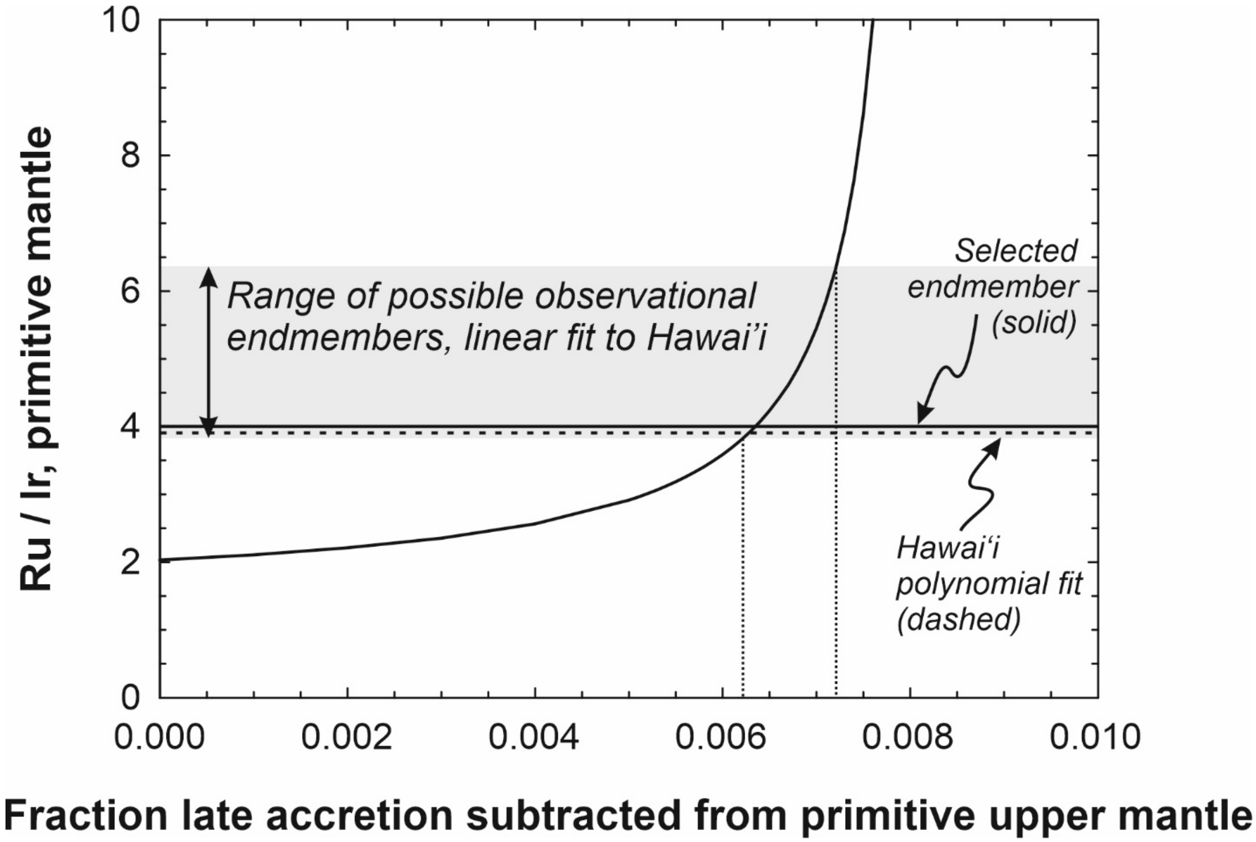

Figure 8. Calculated Ru/Ir ratios for intermediate stages of chondritic late accretion compared to statistical fits for the "OIB mantle" endmember (**Figures 6-7**) from Hawai'i OIB data. An endmember composition of Ru/Ir = 4 is selected based on the polynomial fit to these data ($p = 0.03$, $r^2 = 0.63$ for a second-order polynomial regression) and may represent a post-core formation mantle domain that was depleted in Ir relative to Ru (cf., Laurenz et al., 2016).

References

Alard, O., Griffin, W.L., Lorand, J.P., Jackson, S.E., and O'Reilly, S.Y. (2000) Non-chondritic distribution of the highly siderophile elements in mantle suphides. Nature, 407, 891-894, doi:10.1038/35038049

Arevalo, R.A., and McDonough, W.F. (2008) Tungsten geochemistry and implications for understanding the Earth's interior. Earth and Planetary Science Letters, 272, 656-665.

Ballmer, M.D., Houser, C., Hernlund, J.W., Wentzcovitch, R.M., and Hirose, K. (2017) Persistence of strong silica-enriched domains in the Earth's lower mantle. Nature Geoscience, 10, 236-240.

Becker, H., Horan, M.F., Walker, R.J., Gao, S., Lorand, J.-P., and Rudnick, R.L. (2006) Highly siderophile element composition of Earth's primitive upper mantle: Constraints from new data on peridotite massifs and xenoliths. Geochimica et Cosmochimica Acta, 70, 4528-4550, doi: 10.1016/j.gca.2006.06.004

Blanchard, I., Petitgirard, S., Laurenz, V., Miyajima, N., Wilke, M., Rubie, D.C., Lobanov, S.S., Hennet, L., Morgenroth, W., Tucoulou, R., Bonino, V., Zhao, X., and Franchi, I. (2022) Chemical analysis of trace elements at the nanoscale in samples recovered from laser-heated diamond anvil cell experiments. Physics and Chemistry of Minerals, 49(18), doi: 10.1007/s00269-022-01193-7

Brandon, A.D., and Walker, R.J. (2005) The debate over core-mantle interaction. Earth and Planetary Science Letters, 232, 211-225, doi:10.1016.j.epsl.2005.01.034

Brown, S.M., Elkins-Tanton, L., and Walker, R.J. (2014) Effects of magma ocean crystallization and overturn on the development of ^{142}Nd and ^{182}W isotopic heterogeneities in the primordial mantle. Earth and Planetary Science Letters, 408, 319-330.

Budde, G., Archer, G.J., Tissot, F.L.H., Tappe, S., and Kleine, T. (2022) Origin of the analytical 183W effect and its implications for tungsten isotope analyses. Journal of Analytical Atomic Spectrometry, doi:10.1039/d2ja00102k

Caro, G, Bourdon, B., Birck, J.-L., and Moorbath, S. (2006) High-precision ^{142}Nd/^{144}Nd measurements in terrestrial rocks: Constraints on the early differentiation of the Earth's mantle. Geochimica et Cosmochimica Acta 70, 164-191, doi:10.1016/j.gca.2005.08.015

Chabot, N.L., Wollack, E.A., Humayun, M., and Shank, E.M. (2015) The effect of oxygen as a light element in metallic liquids on partitioning behavior. Meteoritics & Planetary Science, 50(4), 530-546, doi:10.1111/maps.12383

Chazey, W.J., and Neal, C.R. (2005) Platinum-group element constraints on source composition and magma evolution of the Kerguelen Plateau using basalts from ODP Leg 183. Geochimica et Cosmochimica Acta, 69(19), 4685-4701, doi:10.1016/j.gca.2005.02.006

Courtillot, V., Davaille, A., Besse, J., and Stock, J. (2003) Three distinct types of hotspots in Earth's mantle. Earth and Planetary Science Petters, 205, 295-308, doi:10.1016/S0012-821X(02)01048-8

Dale, C.W., Macpherson, C.G., Pearson, D.G., Hammond, S.J., and Arculus, R.J. (2012) Inter-element fractionation of highly siderophile elements in the Tonga Arc due to flux melting of a depleted source. Geochimica et Cosmochimica Acta, 89, 202-225, doi:10.1016/j.gca.2012.03.025

Day, J.M.D. and Brown, D.B. (2021) Ancient melt-depletion in fresh to strongly serpentinized Tonga Trench peridotites. Journal of Petrology, 62(12), 1-23, doi:10.1093/petrology.egab088

Danyushevsky, L.V. and Plechov, P. (2011) Petrolog3: Integrated software for modelling crystallization processes. Geochemistry, Geophysics, Geosystems, 12(7), Q07021, doi:10.1029/2011GC003516

DeFelice, C., Mallick, S., Saal, A.E., and Huang, S. (2019) An isotopically depleted lower mantle component is intrinsic to the Hawaiian mantle plume. Nature Geoscience, 12, 487-492, doi:

Fischer, R.A., Nakajima, Y., Campbell, A.J., Frost, D.J., Harries, D., Langenhorst, F., Miyajima, N., Pollok, K., and Rubie, D.C. (2015) High pressure metal-silicate partitioning of Ni, Co, V, Cr, Si, and O. Geochimica et Cosmochimica Acta, 167, 177-194, doi:10.1016/j.gca.2015.06.026

French, S.W. and Romanowicz, B. (2015) Broad plumes rooted at the base of the Earth's mantle beneath major hotspots. Nature, 525, 95-99, doi:10.1038/nature14876

Frost, D.J., Asahara, Y., Rubie, D.C., Miyajima, N., Dubrovinsky, L.S., Holzapfel, C., Ohtani, E., Miyahara, M., and Sakai, T. (2010) The partitioning of oxygen between the Earth's mantle and core. Journal of Geophysical Research 115, B02202, doi:10.1029/2009JB006302

Gannoun, A., Burton, K.W., Day, J.M.D., Harvey, J., Schiano, P., and Parkinson, I. (2016) Highly siderophile element and Os isotope systematics of volcanic rocks at divergent and convergent plate boundaries and in intraplate settings. Reviews in Mineralogy and Petrology, 81, 651-724, doi:10.2138/rmg.2016.81.11

Hernlund, J.W., and McNamara, A.K. (2015) The core-mantle boundary region, *in* Schubert, G. (ed.), Treatise on Geophysics, 2nd edition, Vol 7, 461-519. Oxford: Elsevier. doi:10.1016/B978-0-444-53802-4.00136-6

Herzberg, C., and Asimow, P.D. (2015) PRIMELT3 MEGA.XLSM software for primary magma calculation: peridotite primary magma MgO contents from the liquidus to the solidus. Geochemistry, Geophysics, Geosystems, 16, 563-578, doi:10.1002/2014GC005631

Herzberg, C., Condie, K., and Korenaga, J. (2010) Thermal history of the Earth and its petrological expression. Earth and Planetary Science Letters, 292, 79-88, doi:10.1016/j.epsl.2010.01.022

Horan, M.F., Walker, R.J., Morgan, J.W., Grossman, J.N., and Rubin, A.E. (2003) Highly siderophile elements in chondrites. Chemical Geology, 196, 5-20, doi:10.1016/S0009-2541(02)00405-9

Horan, M.F., Carlson, R.W., Walker, R.J., Jackson, M., Garçon, M., and Norman, M. (2018) Tracking Hadean processes in modern basalts with 142-Neodymium. Earth and Planetary Science Letters, 484, 184-191, doi:10.1016/j.epsl.2017.12.017

Humayun, M. (2011) A model for osmium isotopic evolution of metallic solids at the core-mantle boundary: Geochemistry Geophysics Geosystems, 12(3), 23 pp.

Ireland, T.J., Walker, R.J., and Garcia, M.O. (2009) Highly siderophile element and ^{187}Os isotope systematics of Hawaiian picrites: implications for parental melt composition and source heterogeneity. Chemical Geology, 260, 112-128.

Jackson, M.G. and Carlson, R.W. (2012) Homogeneous superchondritic ^{142}Nd/^{144}Nd in the mid-ocean ridge basalt and ocean island basalt mantle. Geochemistry Geophysics Geosystems 13, doi:10.1029/2012GC004114.

Jacobsen, S.B., Ranen, M.C., Petaev, M.I., Remo, J.L., O'Connell, R.J., and Sasselov, D.D. (2008) Isotopes as clues to the origin and earliest differentiation history of the Earth. Philosophical Transactions of the Royal Society, 366, 4129-4162, doi:10.1098/rsta.2008.0174

Jamais, M., Lassiter, J.C., and Brügmann, G. (2008) PGE and Os-isotopic variations in lavas from Kohala Volcano, Hawaii: constraints on PGE behavior and melt/crust interaction. Chemical Geology, 250, 16-28.

Keays, R.R. and Lightfoot, P.C. (2007) Siderophile and chalcophile metal variations in Tertiary picrites and basalts from West Greenland with implications for the sulphide saturation history of continental flood basalt magmas. Mineralium Deposita, 42, 319-336, doi:10.1007/s00126-006-0112-4

Kleine, T. and Walker, R.J. (2017) Tungsten isotopes in planets. Annual Review of Earth and Planetary Sciences, 45, 389-417, doi:10.1146/annurev-earth-063016-020037

Laurenz, V., Rubie, D.C., Frost, D.J., and Vogel, A.K. (2016) The importance of sulfur for the behavior of highly-siderophile elements during Earth's differentiation. Geochimica et Cosmochimica Acta, 194, 123-138, doi:10.1016/j.gca.2016.08.012

Li, Z., Leng, K., Jenkins, J., and Cottaar, S. (2022) Kilometer-scale structure on the core-mantle boundary near Hawaii. Nature Communications, 13, 2787, doi:10.1038/s41467-022-30502-5

Lorand, J.-P., Luguet, A., Alard, O., Bezos, A., and Meisel, T. (2008) Abundance and distribution of platinum-group elements in orogenic lherzolites; a case study in a Fonete Rouge lherzolite (French Pyrénées). Chemical Geology, 248, 174-194, doi:10.1016/j.chemgeo.2007.06.030

Ludwig, K.R. (2003) ISOPLOT 3.00. A geochemical toolkit for Microsoft Excel. Berkeley Geocrhonological Center Spec. Publ. No. 4, 70 pp.

Luguet, A., Shirey, S.B., Lorand, J.-P., Horan, M.F., and Carlson, R.W. (2007) Residual platinum-group minerals from highly deopeted harzburgites of the Lherz massif (France) and their role in HSE fractionation of the mantle. Geochimica et Cosmochimica Acta, 71, 3082-3097, doi:10.1016/j.gca.2007.04.011

Marchesi, C., Garrido, C.J., Harvey, J., González-Jiménez, J.M., Hidas, K., Lorand, J.-P., and Gervilla, F. (2013) Platinum-group elements, S, Se and Cu in highly depleted abyssal peridotites from the Mid-Atlantic Ocean Ridge (ODP Hole 1274A): Influence of hydrothermal and magmatic processes. Contributions to Mineralogy and Petrology, 166, 1521-1538, doi:10.1007/s00410-013-0942-x

Mann, U., D.J. Frost, D.C. Rubie, H. Becker and A. Audétat (2012) Partitioning of Ru, Rh, Pd, Re, Ir and Pt between liquid metal and silicate at high pressures and high temperatures – implications for the origin of highly siderophile element concentrations in Earth's mantle: Geochimica et Cosmochimica Acta, 84, 593-613.

Mei, Q.-F., Yang, J.-H., Wang, Y.-F., Wang, H., and Peng, P. (2020) Tungsten isotopic constraints on homogenization of the Archean silicate Earth: Implications for the transition of tectonic regimes. Geochimica et Cosmochimica Acta, 278, 51-64.

Mundl, A., M. Touboul, M.G. Jackson, J.M.D. Day, M.D. Kurz, V. Lekic, R.T. Helz and R.J. Walker (2017) Tungsten-182 heterogeneity in modern ocean island basalts: Science, 356, 66-69.

Mundl, A., Walker, R.J., Reimink, J.R., Rudnick, R.L., and Gaschnig, R.M. (2018) Tungsten-182 in the upper continental crust: Evidence from glacial diamictites. Chemical Geology 494, 144-152.

Mundl-Petermeier, A., Walker, R.J., Jackson, M.G., Blichert-Toft, J., Kurz, M.D., and Haldórsson, S.A. (2019) Temporal evolution of primordial tungsten-182 and ^{3}He/^{4}He signatures in the Iceland mantle plume. Chemical Geology.

Mundl-Petermeier, A., Walker, R.J., Fischer, R.A., Lekic, V., Jackson, M.G., and Kurz, M.D. (2020) Anomalous μ^{182}W signatures in high ^{3}He/^{4}He ocean island basalts – fingerprints of Earth's core? Geochimica et Cosmochimica Acta, 271, 194-211 doi:10.1016/j.gca.2019.12.020

Mungall, J.E. and Brenan, J.M. (2014) Partitioning of platinum-group elements and Au between sulfide liquid and basalt and the origins of mantle-crust fractionation of the chalcophile elements. Geochimica et Cosmochimica Acta, 125, 265-289, doi:10.1016/j.gca.2013.10.002

Norman, M.D. and Garcia, M.O. (1999) Primitive magmas and source characteristics of the Hawaiian plume: petrology and geochemistry of shield picrites. Earth and Planetary Science Letters 168, 27-44, doi:10.1016/S0012-821X(99)00043-6

Otsuka, K. and Karato, S.-i. (2012) Deep penetration of molten iron into the mantle caused by a a morphological instability. Nature, 492, 243-247, doi:10.1038/nature11663

Paquet, M., Day, J.M.D., and Castillo, P.R. (2019) Osmium isotope evidence for a heterogeneous ^{3}He/^{4}He mantle plume beneath the Juan Fernandez Islands. Geochimica et Cosmochimica Acta, 261, 1-19, doi:10.1016/j.gca.2019.06.039

Paquet, M., Day, J.M.D., Brown, D.B., and Waters, C.L. (2022) Effective global mixing of the highly siderophile elements into Earth's mantle inferred by oceanic abyssal peridotites. Geochimica et Cosmochimica Acta, 316, 347-362, doi:10.1016/j.gca.2021.09.033

Peters, B.J., Day, J.M.D., and Taylor, L.A. (2016) Early mantle heterogeneities in the Réunion hotspot source inferred from highly siderophile elements in cumulate xenoliths. Earth and Planetary Science Letters, 448, 150-160, doi:10.1016/j.epsl.2016.05.015

Peters, B.J., Carlson, R.W., Day, J.M.D., and Horan, M.F. (2018) Hadean silicate differentiation preserved by anomalous $^{142}Nd/^{144}Nd$ in the Réunion hotspot source. Nature, 555, 89-93, doi:1.1038/nature25754

Peters, B.J., Mundl-Petermeier, A., Carlson, R.W., Walker, R.J., and Day, J.M.D. (2021) Combined lithophile-siderophile isotopic constraints on Hadean processes preserved in ocean island basalt sources. Geochemistry, Geophysics, Geosystems, 22, e2020GC009479, doi:10.1029/2020GC009479

Peuker-Ehrenbrink, B. and Jahn, B.-m. (2001) Rhenium-osmium systematics and platinum group element concentrations: loess and the upper continental crust. Geochemistry, Geophysics, Geosystems, 2, e2001GC000172, doi:10.1029/2001GC000172

Puchtel, I.S. and Humayun, M. (2001) Platinum group element fractionation in a komatiitic basalt lava lake. Geochimica et Cosmochimica Acta, 65(17), 2979-2993, doi:10.1016/S0016-7037(01)00642-1

Puchtel, I.S., Touboul, M., Blichert-Toft, J., Walker, R.J., Brandon, A.D., Nicklas, R.W., Kulikov, V.S., and Samsonov, A.V. (2016) Lithophile and siderophile element systematics of Earth's mantle at the Archean-Proterozoic boundary: Evidence from 2.4 Ga komatiites. Geochimica et Cosmochimica Acta, 180, 227-255, doi:10.1016/j.gca.2016.02.027

Puchtel, I. S., Blichert-Toft, J., Touboul, M., Horan, M. F., and Walker, R. J. (2016b). The coupled ^{182}W-^{142}Nd record of early terrestrial mantle differentiation. Geochemistry Geophysics Geosystems, 17(6), 2168-2193.

Puchtel, I.S., Mundl-Petermeier, A., Horan, M., Hanski, E.J., Blichert-Toft, J., and Walker, R.J. (2020) Ultra-depleted 2.05 Ga komatiites of Finnish Lapland: Products of grainy late accretion or core-mantle interaction? Chemical Geology, 554, doi:10.1016/j.chemgo.2020.119801

Puchtel, I.S., Blichert-Toft, J., Horan, M.F., Touboul, M., and Walker, R.J. (2022) The komatiite testimony to ancient mantle heterogeneity. Chemical Geology, 594, 120776, doi:10.1016/j.chemgeo.2022.102776

Reimink, J.R., Mundl-Petermeier, A., Carlson, R.W., Shirey, S.B., Walker, R.J., and Pearson, D.G. (2020) Tungsten isotope composition of Archean crustal reservoirs and implications for terrestrial µ182W evolution. Geochemistry, Geophysics, Geosystems, 21, doi:10.1029/2020GC009155

Righter, K., Rowland, R., Danielson, L.R., Humayun, M., Yang, S., Mayer, N., and Pando, K. (2020) Mantle-melt partitioning of the highly siderophile elements: new results and application to Mars. Meteoritics and Planetary Science 55(12), 2741-2757, doi:10.1111/maps.13598

Rizo, H., Walker, R.J., Carlson, R.W., Touboul, M., Horan, M.F., Puchtel, I.S., Boyet, M., Rosing, M.T. (2016) Early Earth differentiation investigated through ^{142}Nd, ^{182}W, and highly siderophile element abundances in samples from Isua, Greenland. Geochimica et Cosmochimica Acta, 175, 319-336, doi:10.1016/j.gca.2015.12.007

Rizo, H., Andrault, D., Bennett, N.R., Humayun, M., Brandon, A., Vlastelic, I., Moine, B., Poirier, A., Bouhifd, M.A., and Murphy, D.T. (2019) ^{182}W evidence for core-mantle interaction in the source of mantle plumes. Geochemical Perspectives Letters, 11, 6-11, doi:10.7185/geochemlet.1917

Rubie, D.C., Frost, D.J., Mann, U., Asahara, Y., Nimmo, F., Tsuno, K., Kegler, P., Holzheid, A., and Palme, H. (2011) Heterogeneous accretion, composition and core-mantle differentiation of the Earth. Earth and Planetary Science Letters, 301, 31-42.

Schmidt, G., Palme, H., and Kratz, K.-L. (1997) Highly siderophile elements (Re, Os, Ir, Ru, Rh, Pd, Au) in impact melts from three European impact craters (Sääksjärvi, Mien, and Dellen): clues to the nature of the impacting bodies. Geochimica et Cosmochimica Acta, 61(14), 2977-2987, doi:10.1016/S0016-7037(97)00129-4

Shofner, G.A., Campbell, A.J., Danielson, L., Rahman, Z., and Righter, K. (2014) Metal-silicate partitioning of tungsten from 10 to 50 GPa. Lunar and Planetary Science Conference Abstracts, 17-21 March 2014, The Woodlands, TX, United States.

Simon, F. and Glatzel, G. (1929) Fusion-pressure curve. Zeitschrift für anorganische und allgemeine Chemie, 178, 309-316.

Suer, T.-A., Siebert, J., Remusat, L., Day, J.M.D., Borensztajn, S., Doisneau, B., and Fiquet, G. (2021) Reconciling metal-silicate partitioning and late accretion in the Earth. Nature Communications, 12, 2913, doi:10.1038/s41467-021-23137-5

Tanaka, R., Nakamura, E., and Takahashi, E. (2002) Geochemical evolution of Koolau volcano, Hawaii. Geophysical Monograph, American Geophysical Union, 128, 311-332, doi:10.1029/GM128p0311

Touboul, M., I.S. Puchtel and R.J. Walker (2012) ^{182}W evidence for long-term preservation of early mantle differentiation products: Science, 355, 1065-1070.

Trønnes, R. (2009) Structure, mineralogy and dynamics of the lowermost mantle. Mineralogy and Petrology, 99, 243-261, doi:10.1007/s00710-009-0068-z

Trønnes, R.G., Baron, M.A., Eigenmann, K.R., Guren, M.G., Heyn, B.H., Løken, A., and Mohn, C.E. (2019) Core formation, mantle differentiation and core-mantle interaction within Earth and the terrestrial planets. Tectonophysics, 760, 165-198, doi:10.1016/j.tecto.2018.10.021

Tusch, J., Sprung, P., van de Löcht, J., Hoffmann, J.E., Boyd, A.J., Rosing, M.T., and Münker, C. (2019) Uniform 182W isotope compositions in Eoarchean rocks from the Isua region, SW Greenland: The role of early silicate differentiation and missing late veneer. Geochimica et Cosmochimica Acta, 257, 284-310, doi:10.1016/j.gca.2019.05.012

Tusch, J., Hoffmann, J.E., Hasenstab, E., Fischer-Gödde, M., Marien, C.S., Wilson, A.H., and Münker, C. (2022) Long-term preservation of Hadean protocrust in Earth's mantle. Proceedings of the National Academy of Science, 119(18), e2120241119, doi:10.1073/pnas.2120241119

Wade, J. and Wood, B.J. (2005) Core formation and the oxidation state of the Earth. Earth and Planetary Science Letters, 236(1-2), 78-95, doi:10.1016/j.epsl.2005.05.017

Walker, R.J. (2009) Highly siderophile elements in the Earth, Moon and Mars: update and implications for planetary accretion and differentiation. Chemie der Erde, 69, 101-125, doi:10.1016/j.chemer.2008.10.001

Waters, C.L., Day, J.M.D., Watanabe, S., Sayit, K., Zanon, V., Olson, K.M., Hanan, B.B., and Widom, E. (2020) Sulfide mantle source heterogeneity recorded in basaltic lavas from the Azores. Geochimica et Cosmochimica Acta, 268, 422-445, doi:10.1016/j.gca.2019.10.012

Weis, D., Harrison, L.N., McMillan, R., and Williamson, N.M.B. (2020) Fine-scale structure of Earth's deep mantle resolved through statistical analysis of Hawaiian basalt geochemistry. Geochemistry, Geophysics, Geosystems, 21, e2020GC009292, doi:10.1029/2020GC009292

Willbold, M., T. Elliott and S. Moorbath (2011) The tungsten isotopic composition of the Earth's mantle before the terminal bombardment: Nature, 477, 195-199.

Yoshino, T., Makino, Y., Suzuki, T., and Hirata, T. (2020) Grain boundary diffusion of W in lower mantle phase with implications for isotopic heterogeneity in oceanic island basalts by core-mantle interactions. Earth and Planetary Science Letters, 530, 115887, doi:10.1016/j.epsl.2019.115887

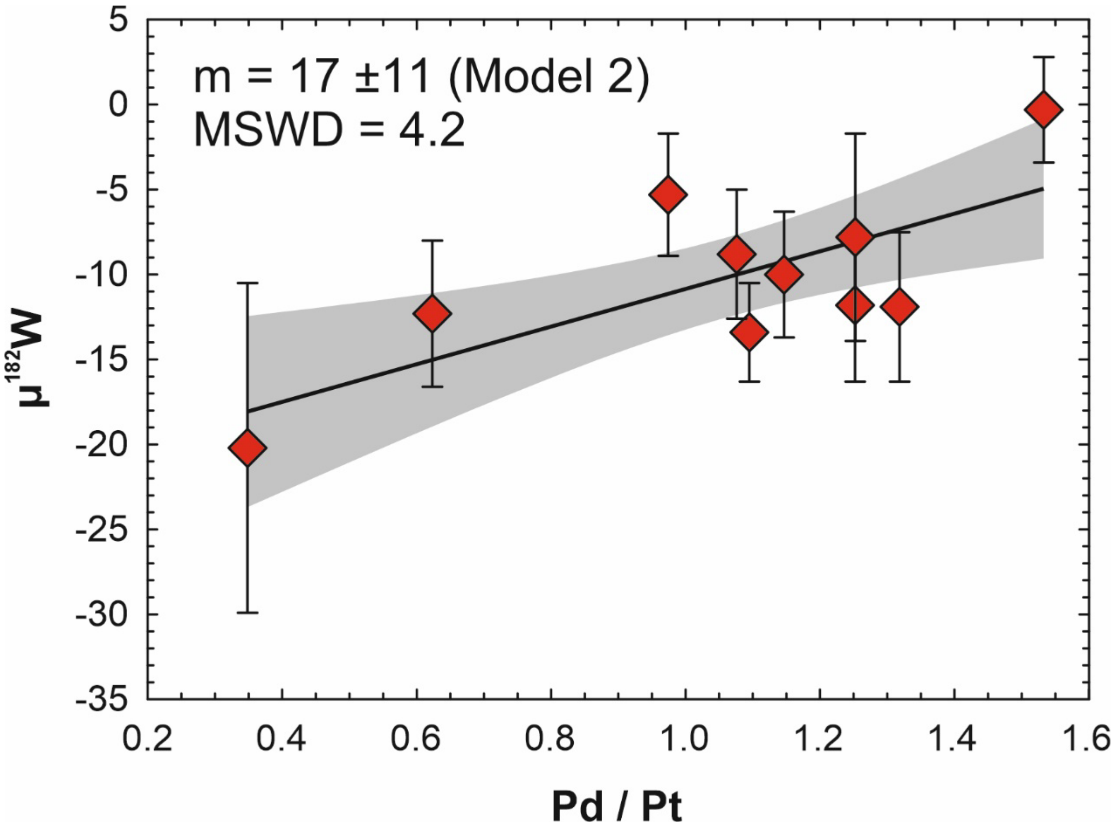

Figure S1. Tungsten isotopic compositions versus Pd/Pt ratios for Hawai‘i OIB. Trend statistics are calculated using Isoplot (Ludwig, 2003); slope uncertainty represents 95% confidence interval of a Model-2 fit.